REPORT

TOPOLOGICAL OPTICS

Engineering spin-orbit synthetic Hamiltonians in liquid-crystal optical cavities

Katarzyna Rechcińska[1]*, Mateusz Król[1]*, Rafał Mazur[2], Przemysław Morawiak[2], Rafał Mirek[1], Karolina Łempicka[1], Witold Bardyszewski[3], Michał Matuszewski[4], Przemysław Kula[5], Wiktor Piecek[2], Pavlos G. Lagoudakis[6,7]†, Barbara Piętka[1], Jacek Szczytko[1]†

Spin-orbit interactions lead to distinctive functionalities in photonic systems. They exploit the analogy between the quantum mechanical description of a complex electronic spin-orbit system and synthetic Hamiltonians derived for the propagation of electromagnetic waves in dedicated spatial structures. We realize an artificial Rashba-Dresselhaus spin-orbit interaction in a liquid crystal–filled optical cavity. Three-dimensional tomography in energy-momentum space enabled us to directly evidence the spin-split photon mode in the presence of an artificial spin-orbit coupling. The effect is observed when two orthogonal linear polarized modes of opposite parity are brought near resonance. Engineering of spin-orbit synthetic Hamiltonians in optical cavities opens the door to photonic emulators of quantum Hamiltonians with internal degrees of freedom.

Spin-orbit interaction (SOI) in atomic and solid-state physics is a relativistic effect transforming static electric fields in the laboratory frame into magnetic fields in the frame of a moving electron. These magnetic fields interact with the spin of the electron and result in a rich variety of quantum phenomena, including the realization of topological states (*1*). SOI in solid-state systems with broken inversion symmetries leads to the so-called Dresselhaus (*2*) and Bychkov-Rashba (*3*, *4*) Hamiltonians that underpin device concepts in spintronics, topological insulators, and superconductors (*5*). SOI effects of light stem directly from the solutions of Maxwell equations in wavelength-scale micro- and nanostructures, including metamaterials, optical waveguides, and interfaces (*6*–*14*), where the role of spin is taken by the polarization of the photons. In the case of a homogeneous medium enclosed in a microcavity, the presence of an energy splitting between transverse electric and transverse magnetic modes of light leads to the optical analog of the spin Hall effect (*15*, *16*) and the realization of artificial gauge fields (*17*, *18*).

[1]Institute of Experimental Physics, Faculty of Physics, University of Warsaw, ul. Pasteura 5, 02-093 Warsaw, Poland. [2]Institute of Applied Physics, Military University of Technology, ul. gen. S. Kaliskiego 2, 00-908 Warsaw, Poland. [3]Institute of Theoretical Physics, Faculty of Physics, University of Warsaw, ul. Pasteura 5, 02-093 Warsaw, Poland. [4]Institute of Physics, Polish Academy of Sciences, al. Lotników 32/46, 02-668 Warsaw, Poland. [5]Institute of Chemistry, Military University of Technology, ul. gen. S. Kaliskiego 2, 00-908 Warsaw, Poland. [6]Skolkovo Institute of Science and Technology, Skolkovo 143025, Russian Federation. [7]Department of Physics and Astronomy, University of Southampton, Southampton SO17 1BJ, UK.
*These authors contributed equally to this work.
†Corresponding author. Email: p.lagoudakis@skoltech.ru (P.G.L.); jacek.szczytko@fuw.edu.pl (J.S.)

The Hamiltonian of a charged particle in a magnetic field is known to be simulated by certain photonic systems with induced gauge fields (*19*–*22*). In these devices, the vector potentials describing the gauge fields are spin-independent, and so the particle's internal degree of freedom remains unaffected. The coupling between potential and spin has been realized, for example, in metamaterials (*23*, *24*). However, the study of artificial Rashba-Dresselhaus spin-orbit gauge fields has been so far predominantly restricted to nanokelvin temperatures in atomic systems (*25*, *26*).

Here, we simulate spin-orbit interactions in a tunable, liquid crystal (LC)–filled, optical cavity. By controlling the refractive index anisotropy of the intracavity layer, we adiabatically engineer the coupling between optical modes and show that the system is described by a Hamiltonian with Dresselhaus (*2*) and Bychkov-Rashba (*3*, *4*) terms, originally used to describe fermions. We fabricated a two-dimensional (2D) capacitive planar multimode optical cavity and filled it with a birefringent LC medium in the nematic state, as shown in Fig. 1A (*27*). By applying an external voltage, we controlled the spatial orientation of the long molecular axis of the LC medium that induces refractive index anisotropy. The refractive index anisotropy in the *xy* plane can be described using ordinary n_o and extraordinary n_e refractive indices. At normal incidence, for a cavity mode with l antinodes, this leads to an energy splitting between the two orthogonal linearly polarized cavity modes, with energies denoted by $E_{X,l}$ and $E_{Y,l}$. By rotating the optical axis of the LC medium around the y axis, shown in Fig. 1A, we control the effective refractive index relevant to the electric field oscillating in the *xz* plane, and thus the energy of the *X*-polarized modes (*28*). This configuration enables us to utilize the giant optical anisotropy of the LC medium [$\Delta n = n_e - n_o = 0.41$ (*29*)] and bring successive modes into resonance.

When two orthogonally polarized cavity modes of opposite parity of the number of antinodes l and l' are tuned near resonance, a coupling between them arises, which depends on the in-plane wave vector of incident light, denoted as $\mathbf{k}_\parallel = (k_x, k_y)$. The coupling term is analogous to the Rashba-Dresselhaus Hamiltonian with equal strength of Rashba and Dresselhaus couplings (*30*), $\hat{H}_{\mathrm{RD}} = -2\alpha\hat{\sigma}_z k_y$, where $\hat{\sigma}_z$ is the third Pauli matrix (defined in the basis of circular polarizations of out-coupled light $\sigma^{\pm}$ at the LC, Bragg mirror interface, as shown in Fig. 1B) and α is the Rashba-Dresselhaus coupling coefficient. This form of the Rashba-Dresselhaus coupling term can be deduced from the symmetry of the system (*27*).

The quasi-degenerate system of the orthogonally polarized modes of opposite parity can be approximately described by the effective Hamiltonian

$$\hat{H} = \frac{\hbar^2 k_x^2}{2m_x} + \frac{\hbar^2 k_y^2}{2m_y} + \hat{H}_{\mathrm{RD}} + \frac{1}{2}(E_{X,l} - E_{Y,l'})\hat{\sigma}_x \quad (1)$$

where m_x and m_y are the effective masses of the cavity photon in the *xy* plane (compare to Figure 1A), and $\hbar$ is Planck's constant h divided by 2π. The first two terms correspond to the kinetic energy of cavity photons, that is, photon confinement in the z direction results in a parabolic dispersion relation with respect to $\mathbf{k}_\parallel$, or the photon in-plane momentum. The third term corresponds to the Rashba-Dresselhaus coupling with a gauge field defined as $\hat{\mathbf{A}} = 2m_y\hat{\sigma}_z/\hbar(0,1,0)$. The Rashba-Dresselhaus coupling gives rise to two cross-circular polarized eigenstates separated in momentum space shown in Fig. 1C. Constant energy cross-sections of the 3D paraboloid are shown in Fig. 1D. The last term in the Hamiltonian (Eq. 1) corresponds to the splitting between the cavity eigenmodes $E_{X,l}$ and $E_{Y,l'}$ that acts as an artificial magnetic field in the x direction, resulting in a synthetic Zeeman term for the spin but not the orbital degree of freedom (*31*).

Under oblique incidence, the eigenmodes are neither *X* nor *Y* polarized because $\mathbf{k}_\parallel \neq 0$. At resonance, the phase difference between the *X*- and *Y*-polarization modes across the intracavity LC layer changes by π. The intracavity LC layer acts, then, as a half-wave plate, and the eigenmode polarization at the mirror interfaces becomes circular; thus, out-coupled light is circularly $\sigma^{\pm}$ polarized, with the same polarization on both sides of the cavity, as shown in Fig. 1B.

The lifted degeneracy of $\sigma^{\pm}$ polarizations (Fig. 1C) and the asymmetric cross section

in reciprocal space (Fig. 1D) of the Rashba-Dresselhaus coupled photons appear to break time-reversal (TR) symmetry in a purely photonic system. Paradoxically, the possibility to realize synthetic Rashba-Dresselhaus spin-orbit coupling for photons in such a simple system can be precisely justified by considering the effect of TR symmetry on confined photon modes. As shown in Fig. 1E, TR of a ($\mathbf{k}$, $\sigma^{\pm}$) circularly polarized electromagnetic wave in free space results in an electromagnetic wave with opposite momentum $-\mathbf{k}$ and the same polarization. Consequently, in a TR symmetric system, a plane wave spectrum is always symmetric with respect to inversion of momentum $\mathbf{k}$. However, such a symmetry argument does not hold for cavity modes parameterized with momentum in the plane of the cavity because ($\mathbf{k}_{\parallel}$, $\sigma^{\pm}$) and ($-\mathbf{k}_{\parallel}$, $\sigma^{\pm}$) are not TR symmetric partners. Indeed, reflection of circularly polarized light flips both the sign of the component of the wave vector perpendicular to the mirror, $\mathbf{k}_{\perp}$, and the polarization, $\sigma^{\mp}$, as shown schematically in Fig. 1, F and G. Therefore, modes ($\mathbf{k}_{\parallel}$, $\mathbf{k}_{\perp}$, $\sigma^{\pm}$) and ($\mathbf{k}_{\parallel}$, $-\mathbf{k}_{\perp}$, $\sigma^{\mp}$) couple in the cavity and form a standing wave. Thus, TR in the cavity transforms ($\mathbf{k}_{\parallel}$, $\mathbf{k}_{\perp}$, $\sigma^{\pm}$) into ($-\mathbf{k}_{\parallel}$, $\mathbf{k}_{\perp}$, $\sigma^{\mp}$), that is, $\mathbf{k}_{\parallel} \rightarrow -\mathbf{k}_{\parallel}$ and $\sigma^{\pm} \rightarrow \sigma^{\mp}$. This permits asymmetric spectra in both $\sigma^{\pm}$ polarizations that result in the apparent symmetry "breaking" with respect to $k = 0$, reminiscent to that of fermionic spin-$\frac{1}{2}$ particles (*27*).

To experimentally realize the manifestation of the Rashba-Dresselhaus coupling, we perform polarization-resolved reflectivity measurements in reciprocal space. We use a broadband incoherent source to eliminate coherent artifacts. In the absence of an external voltage (first row of Fig. 2), the director of the LC medium is parallel to the cavity plane, pointing in the x direction. In this configuration, we expect a large energy splitting between the X- and Y-polarization modes. The 2D polarization-resolved dispersion of the cavity photons consists of coaxial paraboloids shown in Fig. 2A, where we can clearly observe two successive cavity modes. Figure 2B shows the corresponding reflectivity dispersion at the $k_x = 0$ cross section. Polarization-resolved reflectivity of the dispersion along the X- and Y-polarization modes allows us to distinguish the relevant modes. Figure 2C shows the dispersion of the degree of linear polarization (DLP) at the $k_x = 0$ cross section of the 2D dispersion. The two orthogonal modes correspond to the main axes of the LC indicatrix.

Application of an external voltage on the electrodes of the cavity allows for a smooth tuning of the energy of the X-polarized paraboloid. At 1.38 V, two orthogonally polarized modes of the same parity are brought into a resonance at normal incidence (second row of Fig. 2). Figure 2D shows the 2D polarization-resolved dispersion, and Fig. 2E shows the corresponding reflectivity dispersion at the $k_x = 0$ cross section. The two modes have slightly different curvature (effective masses) in the k_y direction owing to the residual alignment of the LC director; naturally, the cross section at the k_x direction (left projection of Fig. 2D) does not exhibit any difference. The

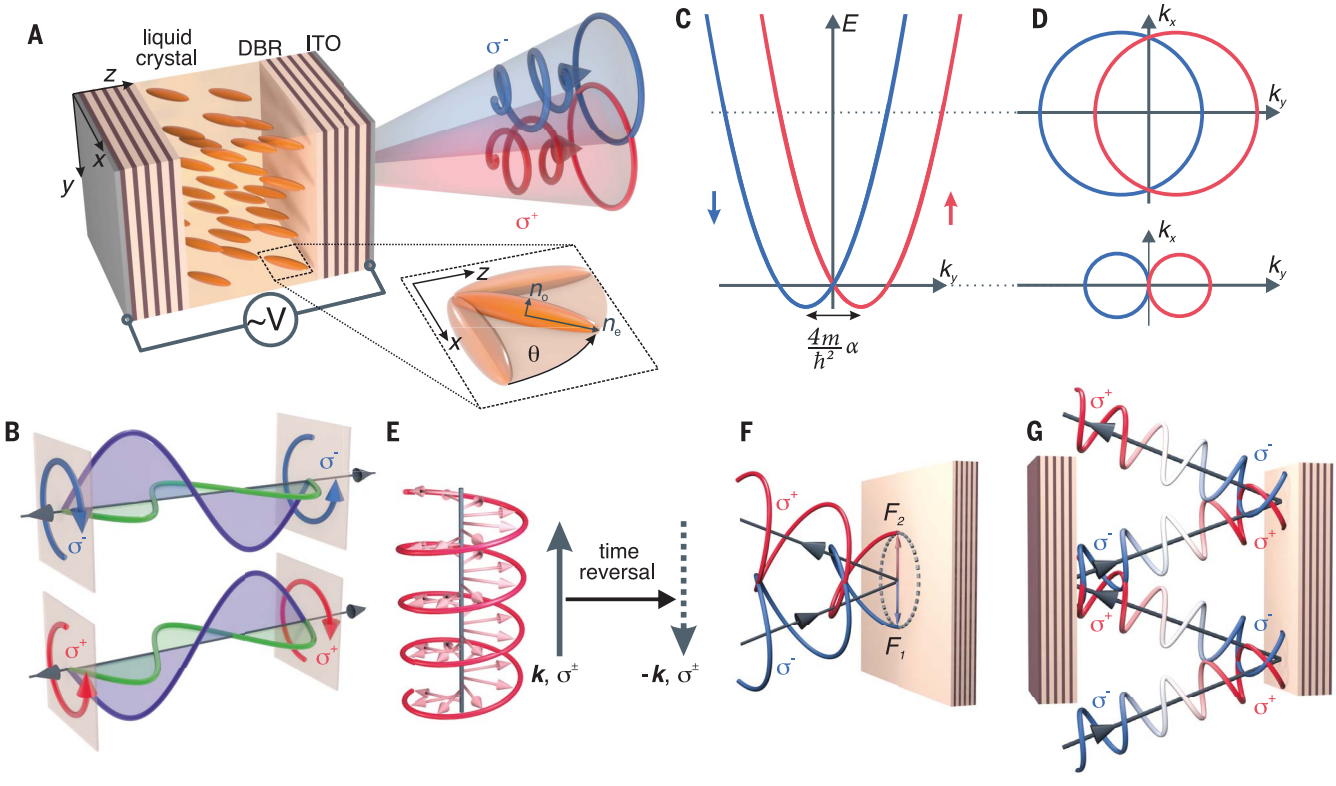

Fig. 1. Rashba-Dresselhaus spin-orbit coupling in a liquid crystal–filled optical cavity. (**A**) Scheme of the LC-filled optical cavity made of two distributed Bragg reflectors (DBRs) with ac source (V) connected to indium tin oxide (ITO) electrodes. (**B**) Resonant X- and Y-polarization modes of opposite parities l and l'; the LC medium acts as a half-wave plate, and the eigenmode polarization at the mirror interfaces becomes circular. Out-coupled light is circularly polarized with the same ($\sigma^{\pm}$) polarization on either side of the cavity. (**C**) Dispersion relation with spin-polarized bands resulting from Rashba-Dresselhaus coupling. (**D**) Constant energy cross sections in k_{xy} reciprocal space. (**E**) Circularly polarized beam under TR switches its propagation direction, but the chirality remains the same. In a TR symmetric system, this results in $\mathbf{k}$-symmetric spectra for all polarizations. (**F**) Mirror reflection switches both the perpendicular part of the momentum and the chirality of the incident beam, as the sum of the incident (F_1) and reflected (F_2) electric fileds at interface is equal to zero. (**G**) In the cavity, both ($\mathbf{k}_{\parallel}$, $\mathbf{k}_{\perp}$, $\sigma^{\pm}$) and ($\mathbf{k}_{\parallel}$, $-\mathbf{k}_{\perp}$, $\sigma^{\mp}$) modes couple with each other to form a standing wave. Under TR, both the wave vector parallel to the cavity plane and circular polarization change sign, $\mathbf{k}_{\parallel} \rightarrow -\mathbf{k}_{\parallel}$ and $\sigma^{\pm} \rightarrow \sigma^{\mp}$, resulting in symmetry breaking of the intracavity circularly polarized modes.

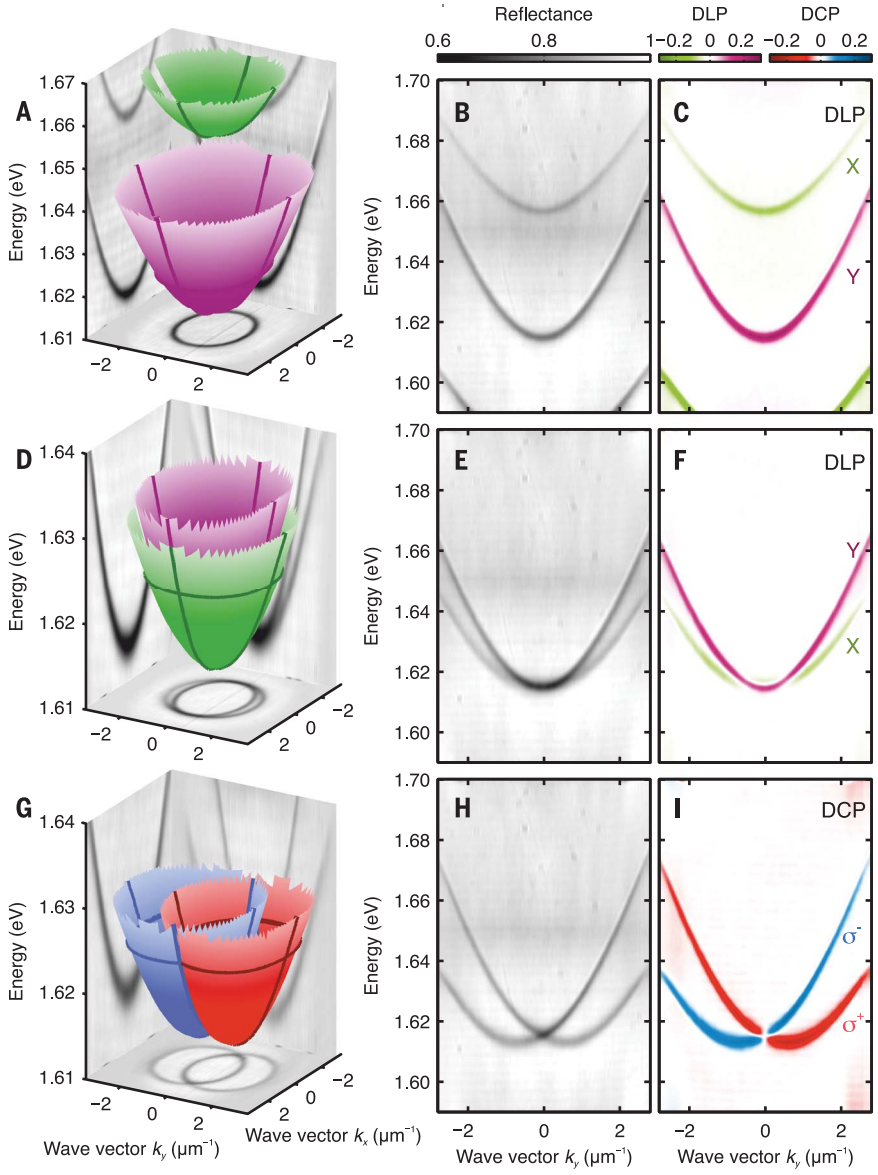

Fig. 2. Dispersion engineering in a tunable liquid crystal–filled optical cavity. (**A**, **D**, and **G**) Experimental 2D polarization-resolved reciprocal space tomography of reflectance at 0.0 (A), 1.38 (D), and 2.48 V (G). (**B**, **E**, and **H**) Reflectance dispersion at the k_x = 0 cross section. (**C** and **F**) The dispersion of the DLP at the k_x = 0 cross section of the respective 2D dispersions for modes of the same parity. The two orthogonal modes correspond to the main axes of the LC indicatrix. (**I**) The dispersion of the DCP at the k_x = 0 cross section of the 2D dispersion, realizing the solution of the Rashba-Dresselhaus Hamiltonian of Fig. 1C.

dispersion of the degree of linear polarization at the k_x = 0 cross section of the 2D dispersion, shown in Fig. 2F, reveals that the two modes maintain their polarization.

For an even higher external bias of 2.48 V, we bring into resonance two orthogonally polarized modes of opposite parity (third row of Fig. 2). Figure 2G shows the 2D polarization-resolved dispersion, analyzed in the circular polarization basis. Here, we observe a clear splitting of the paraboloids in the k_y direction. Figure 2H shows the corresponding reflectivity dispersion at the k_x = 0 cross section. The dispersion of the degree of circular polarization (DCP) at the k_x = 0 cross section of the 2D dispersion, shown in Fig. 2I, reveals the Rashba-Dresselhaus Hamiltonian solution of Fig. 1C.

The emergence of the coupling between the modes can be precisely traced on the reflectivity dispersion as a function of the applied voltage. In Fig. 3A, we plot the reflectivity spectrum versus applied voltage at normal incidence (k_y = 0) for the range of voltages, wherein we observe crossing of the resonances of two orthogonal polarization modes with

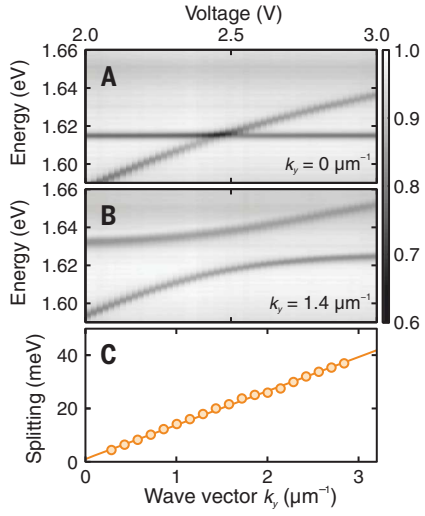

Fig. 3. Giant Rashba coupling in an optical cavity. (**A** and **B**) Reflectance (color scale) at k_y = 0 (A) and k_y = 1.4 μm^{-1} (B) versus applied voltage. (**C**) Energy-mode splitting between the cavity eigenmodes $E_{X,I}$ and $E_{Y,I}$ versus in-plane wave vector k_y at 2.48 V. From the slope of a linear fit to the data, we obtain a giant Rashba-Dresselhaus parameter of α = 31.9 eV·Å.

opposite parity. At normal incidence, we observe a clear crossing of the two modes, in agreement with the Rashba-Dresselhaus coupling term. In Fig. 3B, we plot the reflectivity spectrum versus applied voltage at k_y = 1.4 μm^{-1}. In this case, we observe a clear anticrossing at the resonance conditions for the two modes. This is in agreement with the Rashba-Dresselhaus coupling term that is linear on in-plane wave vector (k_y). Tuning the applied voltage, we determined the splitting as a function of the wave vectors (Fig. 3C). From the slope of the linear dependence of the energy splitting on k_y, we obtained a giant Rashba-Dresselhaus parameter of α = 31.9 eV·Å.

We demonstrate a photonic device that realizes a tunable synthetic Hamiltonian consisting of the Rashba-Dresselhaus and Zeeman terms. Synthetic Hamiltonians enable the study of physical systems, wherein tunable gauge fields and forces play an important role. Utilizing pure bosons to engineer the Rashba-Dresselhaus Hamiltonian allows for the emulation of physical systems with SOI and microscale control over spin states, for example, persistent spin helix (*30*), suppression of spin relaxation (*32*), and creation of topologically protected states of light (*33*). Such artificial gauge fields can be further applied to light-matter dressed states, bringing about an exotic Hamiltonian with intrinsic nonlinearities.

REFERENCES AND NOTES

1. M. Z. Hasan, C. L. Kane, *Rev. Mod. Phys.* **82**, 3045–3067 (2010).
2. G. Dresselhaus, *Phys. Rev.* **100**, 580–586 (1955).

3. E. I. Rashba, V. I. Sheka, *Fiz. Tverd. Tela: Collected Papers* **2**, 162 (1959).
4. Y. A. Bychkov, E. Rashba, *JETP Lett.* **39**, 78 (1984).
5. A. Manchon, H. C. Koo, J. Nitta, S. M. Frolov, R. A. Duine, *Nat. Mater.* **14**, 871–882 (2015).
6. V. S. Liberman, B. Y. Zel'dovich, *Phys. Rev. A* **46**, 5199–5207 (1992).
7. K. Y. Bliokh, F. J. Rodríguez-Fortuño, F. Nori, A. V. Zayats, *Nat. Photonics* **9**, 796–808 (2015).
8. F. Cardano, L. Marrucci, *Nat. Photonics* **9**, 776–778 (2015).
9. K. Y. Bliokh, *J. Opt. A, Pure Appl. Opt.* **11**, 094009 (2009).
10. K. Y. Bliokh, D. Smirnova, F. Nori, *Science* **348**, 1448–1451 (2015).
11. M. Onoda, S. Murakami, N. Nagaosa, *Phys. Rev. Lett.* **93**, 083901 (2004).
12. K. Y. Bliokh, Y. Gorodetski, V. Kleiner, E. Hasman, *Phys. Rev. Lett.* **101**, 030404 (2008).
13. A. Aiello, N. Lindlein, C. Marquardt, G. Leuchs, *Phys. Rev. Lett.* **103**, 100401 (2009).
14. K. Y. Bliokh, C. Prajapati, C. T. Samlan, N. K. Viswanathan, F. Nori, *Opt. Lett.* **44**, 4781–4784 (2019).
15. A. Kavokin, G. Malpuech, M. Glazov, *Phys. Rev. Lett.* **95**, 136601 (2005).
16. C. Leyder *et al.*, *Nat. Phys.* **3**, 628–631 (2007).
17. H. Terças, H. Flayac, D. D. Solnyshkov, G. Malpuech, *Phys. Rev. Lett.* **112**, 066402 (2014).
18. A. Gianfrate, O. Bleu, Direct measurement of the quantum geometric tensor in a two-dimensional continuous medium. arXiv:1901.03219v1 [cond-mat.mes-hall] (10 January 2019).
19. M. Aidelsburger, S. Nascimbene, N. Goldman, *C. R. Phys.* **19**, 394–432 (2018).
20. H.-T. Lim, E. Togan, M. Kroner, J. Miguel-Sanchez, A. Imamoğlu, *Nat. Commun.* **8**, 14540 (2017).
21. Z. Wang, Y. Chong, J. D. Joannopoulos, M. Soljačić, *Nature* **461**, 772–775 (2009).
22. M. C. Rechtsman *et al.*, *Nat. Photonics* **7**, 153–158 (2012).
23. N. Shitrit *et al.*, *Science* **340**, 724–726 (2013).
24. Y. Lumer *et al.*, *Nat. Photonics* **13**, 339–345 (2019).
25. Y.-J. Lin, K. Jiménez-García, I. B. Spielman, *Nature* **471**, 83–86 (2011).
26. V. Galitski, I. B. Spielman, *Nature* **494**, 49–54 (2013).
27. See supplementary materials.
28. K. Lekenta *et al.*, *Light Sci. Appl.* **7**, 74 (2018).
29. E. Miszczyk *et al.*, *Liq. Cryst.* **45**, 1690–1698 (2018).
30. B. A. Bernevig, J. Orenstein, S.-C. Zhang, *Phys. Rev. Lett.* **97**, 236601 (2006).
31. D. Solnyshkov, G. Malpuech, *C. R. Phys.* **17**, 920–933 (2016).
32. J. D. Koralek *et al.*, *Nature* **458**, 610–613 (2009).
33. D. Leykam, K. Y. Bliokh, C. Huang, Y. D. Chong, F. Nori, *Phys. Rev. Lett.* **118**, 040401 (2017).

ACKNOWLEDGMENTS

Funding: This work was supported by the Ministry of Higher Education, Poland, under project "Diamentowy Grant" 0005/DIA/2016/45 and 0109/DIA/2015/44; National Science Centre grants 2016/23/B/ST3/03926, 2017/27/B/ST3/00271, 2016/22/E/ST3/00045, and 2018/31/N/ST3/03046; the Ministry of National Defense Republic of Poland Program, Research Grant MUT Project 13–995; and UK Engineering and Physical Sciences Research Council grant EP/M025330/1 on Hybrid Polaritonics. **Author contributions:** K.R., M.K., R.Mi., and K.Ł. performed the experiments under the guidance of B.P. and J.S. P.K. synthesized liquid crystal. R.Ma., P.M., and W.P. constructed and fabricated the LC microcavity. W.B. and M.M. worked on the theoretical description. W.B. developed the waveguide approximation. M.M. determined polarizations on the Poincare sphere. All authors participated in the interpretation of experimental data. J.S., B.P., W.P., and P.G.L. supervised the project, and J.S. was a head of the project. P.G.L., J.S., M.K., and K.R. wrote the manuscript with input from all other authors. **Competing interests:** The authors declare no competing interests. **Data and materials availability:** All data are available in the main text or supplementary materials.

SUPPLEMENTARY MATERIALS

science.sciencemag.org/content/366/6466/727/suppl/DC1
Materials and Methods
Supplementary Text
Figs. S1 to S21
Table S1
References (*34*–*38*)

18 June 2019; accepted 15 October 2019
10.1126/science.aay4182

Science

Engineering spin-orbit synthetic Hamiltonians in liquid-crystal optical cavities

Katarzyna Rechcinska, Mateusz Król, Rafal Mazur, Przemyslaw Morawiak, Rafal Mirek, Karolina Lempicka, Witold Bardyszewski, Michal Matuszewski, Przemyslaw Kula, Wiktor Piecek, Pavlos G. Lagoudakis, Barbara Pietka and Jacek Szczytko

Science **366** (6466), 727-730.
DOI: 10.1126/science.aay4182

Inducing optical spin-orbit coupling

The coupling of the spin-orbit interactions in solid-state systems can give rise to a wide range of exotic electronic transport effects. But solid-state systems tend to be somewhat limited in their flexibility because the spin-orbit coupling is fixed. By contrast, optical systems have recently been shown to mimic complex solid-state systems, with flexibility in d esign providing the ability to control and manipulate the system properties. Using a liquid crystal–filled photonic cavity, Rechcinska *et al.* emulated an artificial Rashba-Dresselhaus spin-orbit coupling in a photonic system and showed control of an artificial Zeeman splitting. The results illustrate a powerful approach of engineering synthetic Hamiltonians with photons for the simulation of nontrivial condensed matter and quantum phenomena.

Science, this issue p. 727